Transferring Momentum into Vacuum

Torsion Balance Tests and FEM

Abstract:

Torsion Balance tests and FEM hint that, given a specific magnetic field geometry, there may exist a possibility of transferring momentum to-and-from the transient pairs that are part of vacuum fluctuations.

The tests for magnet assembly where there was no expected interaction with the transient particles (noQF configurations) are in close agreement with FEM modelling.
The tests with the magnets configured in a way that such interaction was expected, did not agree with modeling and showed a force that was NOT proportional to the Compass-Angle. Across seven runs the antisymmetric (left/right) residual was negative in six and near zero in the qualifying null run, clustering at 2–3 μN, with a sign that matches the field geometry in the FEM model. This component is reproducible in sign; its magnitude is not yet pinned down, and in Earth's field it cannot be separated from conventional field coupling. The primary baseline-qualified result (Runs 2, 3, 5, 8) is −2.06 ± 2.17 μN (nominal 95 % run-to-run interval, [−4.23, +0.11]), consistent with zero and still subject to unresolved common-calibration and configuration-dependent-coupling systematics. I therefore report it as a reproducible, configuration-dependent residual of a few μN — not a proof of the hypothesis — and propose a field-nulling experiment to test it.

Introduction:

Can a non uniform magnetic fields create conditions under which momentum exchange with the vacuum becomes detectable?

Static magnetic fields are not expected to produce net forces in vacuum. In classical electrodynamics, a closed magnetic system cannot generate thrust without interacting with external matter or fields. In quantum field theory (QFT), vacuum fluctuations are Lorentz invariant and do not provide a preferred direction for momentum exchange.

Several well-established phenomena, all with explicit boundary conditions, demonstrate that the vacuum is not inert:

- the Casimir effect, where vacuum energy depends on geometry [1],
- the Dynamical Casimir Effect, where vacuum fluctuations convert into real photons [2],
- vacuum polarization in strong fields [4],
- the Unruh and Hawking effects, where observers disagree on vacuum particle content [5,6].

A word of caution:

This work is in no way conclusive; it requires broad independent validation.

Classical field-coupling and QF results are identical in Earth's field

© 2026 Mikolaj Baczynski mikolaj.bzk@gmail.com

Links and References

README.txt on my google drive where you can find description and Excel files including details of all experiments:

- https://drive.google.com/drive/folders/1kyX9nqq-aMQAfwHtXjgVs02RM9rtdCLb?usp=drive_link

Papers describing the "failed" experiments:

- Beam Balance https://www.academia.edu/126856455/Transfering_momentum_into_vacuum
- Pendulum https://www.academia.edu/164472028/Transferring_momentum_into_vacuum_Pendulum_Testing

References:

[1] H. B. G. Casimir, "On the attraction between two perfectly conducting plates," *Proc. K. Ned. Akad. Wet.*, 1948.

[2] C. M. Wilson et al., "Observation of the dynamical Casimir effect in a superconducting circuit," *Nature*, 2011.

[3] G. Moddel et al., "Zero-point energy extraction experiments," various publications.

- "Zero-Point Energy: Capturing Evanescence." Garret Moddel, Journal of Scientific Exploration 36(3) 493-503 (2022). doi.org/10.31275/20222567 https://journalofscientificexploration.org/index.php...

[4] J. Schwinger, "On gauge invariance and vacuum polarization," *Phys. Rev.*, 1951.

[5] W. G. Unruh, "Notes on black-hole evaporation," *Phys. Rev. D*, 1976.

[6] S. W. Hawking, "Particle creation by black holes," *Commun. Math. Phys.*, 1975.

Gravity as zero-point fluctuation force:

- https://www.researchgate.net/publication/13386630....
- https://journals.aps.org/pra/abstract/10.1103/PhysRevA.44.3379

© 2026 Mikolaj Baczynski mikolaj.bzk@gmail.com

Page Links

4. The Underlying Thought Experiment

5. Setup Details

6. Calibration Example: Lead Weight Tests

7. Calculating the Twisting Force

8. Analysis of Test configurations

9. Testing with Single Magnet Configurations

10. Force Analysis

11. Estimating the Force due to the Earth's magnetic field

12. Vertical Component of the Earth's magnetic field

13. Estimating interaction with Earth's magnetic field using FEM

14. FEM: comparison of methods

15. Estimating the Force due to environmental contamination

16. Errors due to Assembly Placement

17. Open-ended, Shielded Configuration

18. Mu-metal, Shunting Not Shielding

19. Estimating QF Based on Test Results

20. Comparison of QF Detection Methods

21. Beam Calibration Results

22. Main Test Results, Method C

23. Main Test Results, Method B

24. Main Test Results, Method A

25. Test Run Variations

26. Test Run Summary

27. Conclusions

28. Vacuum Energy (Event Analysis)

29. Vacuum Energy (estimating QF)

30. Vacuum Energy (assumptions) Speculative Engineering Approach

31. Field Nulling with Helmholtz Coils (still to be performed)

32. Design Details of Helmholtz Coils

© 2026 Mikolaj Baczynski mikolaj.bzk@gmail.com

The Underlying Thought Experiment

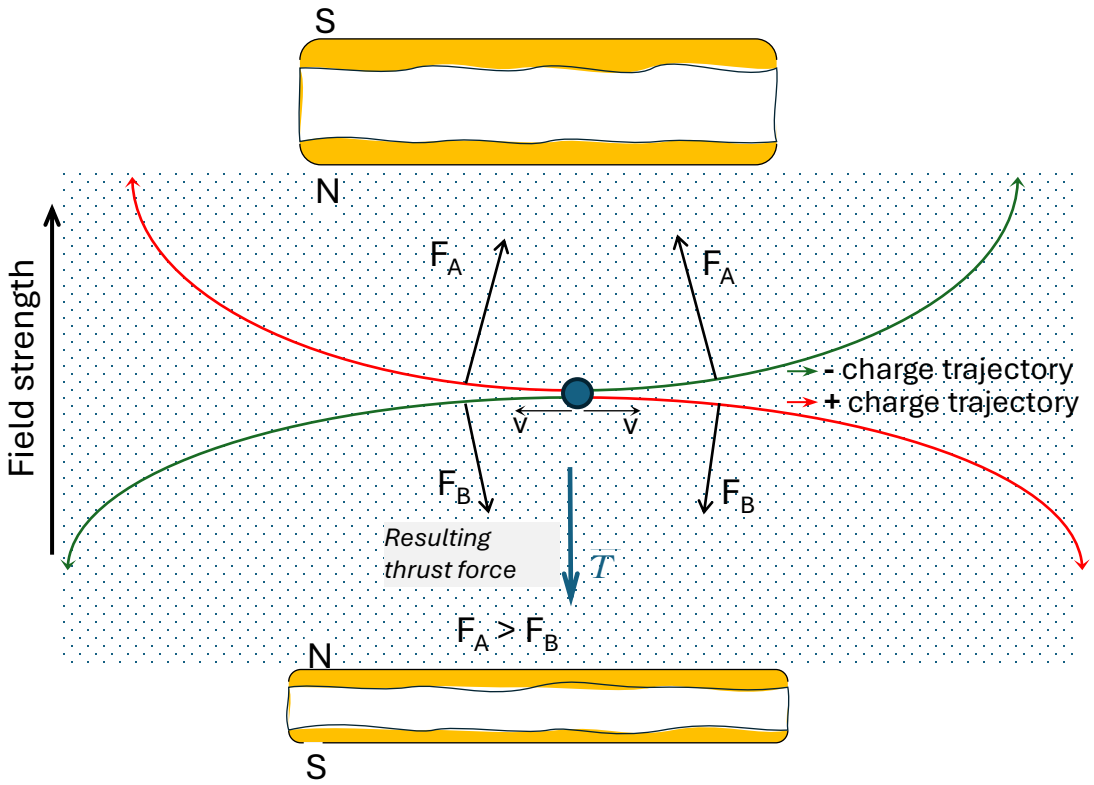

Figure 1. Trajectories of charged particles in non uniform magnetic field

Figure 1. describes the trajectories of particle-antiparticle pairs in non-uniform magnetic field:

- With the strength magnetic field varying as shown, positive-negative pair will be pushed with a different force than the negative-positive pair because the strength of the magnetic field increases along the trajectory of the positive-negative pair and decreases along the trajectory of the negative-positive pair
- Given that F_A is > than F_B we should expect a force acting on the magnets
- Moving the magnet assembly results in transfer of momentum into vacuum

Note:

There is no support in the Current Physics for Figure 1.

Experiments that do show vacuum momentum transfer are fundamentally different from static magnet gradients. They involve:

- time-dependent boundaries
- moving mirrors
- radiation emission

© 2026 Mikolaj Baczynski mikolaj.bzk@gmail.com

Setup Details

Schematic View

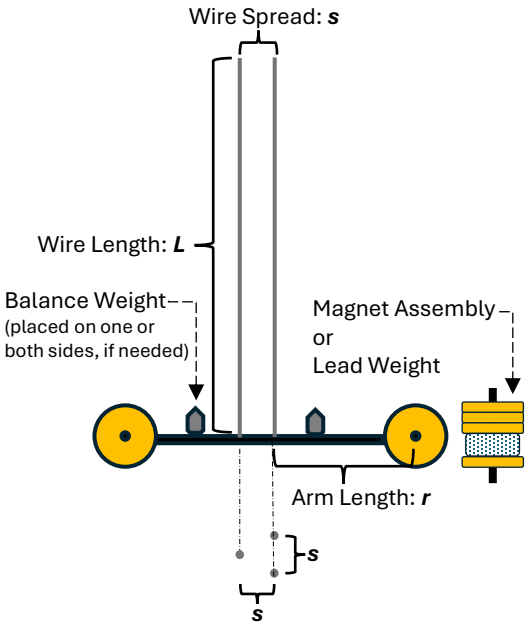

Measurement Setup (Top view)

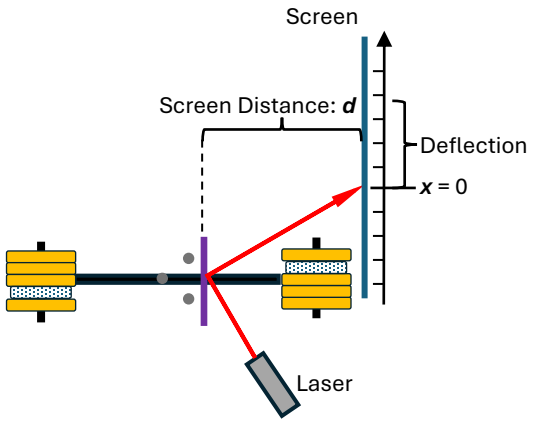

Wire length ***L***	- 1.04[m]
Arm Length ***r***	- 0.40[m]
Wire Spread ***s***	- 0.03]m]
Screen Distance ***d***	- see test details
Reflection Offset ***e***	- see test details

Masses:

• Beam	- 57[g]
• Magnet Assembly	- 105.7[g]
• Lead Weight	- 6.9[g]
• Balance Weight	- 101.4[g]

Deflection:

- Measured vs Lead Weights configuration

Moment of inertia:

• Beam:	0.00304; (1/12)*(57g)*(0.8m)^2
• Lead Weights:	0.03245; 2*(101.4g)*(0.4m)^2
• **Total:**	0.0355[kg*m^2]; 0.03245 + 0.00304
• Magnets:	0.0338; 2*(105.7g)*(0.4m)^2
• **Total:**	0.0369[kg*m^2]; 0.0338 + 0.00304

© 2026 Mikolaj Baczynski mikolaj.bzk@gmail.com

Calibration Example: Lead Weight Tests

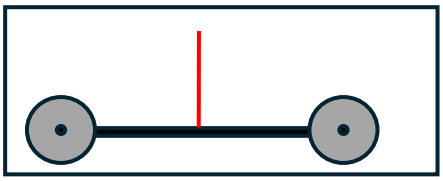

Timestamp (mm:ss.ms)	Event #	Diff	Avg Diff
25:09.539	1		
25:53.023	2	00:43.484	00:43.484
26:36.445	3	00:43.422	00:43.453
27:19.867	4	00:43.422	00:43.443
28:03.429	5	00:43.562	00:43.473
28:46.867	6	00:43.438	00:43.466
29:30.117	7	00:43.250	00:43.430
30:13.804	8	00:43.687	00:43.466
30:57.210	9	00:43.406	00:43.459
31:40.664	10	00:43.454	00:43.458
32:24.085	11	00:43.421	00:43.455
33:07.703	12	00:43.618	00:43.469
33:50.992	13	00:43.289	00:43.454
34:34.632	14	00:43.640	00:43.469
35:17.742	15	00:43.110	00:43.443
36:01.187	16	00:43.445	00:43.443
36:44.726	17	00:43.539	00:43.449
37:28.210	18	00:43.484	00:43.451

Oscillation Period
- Event # - measurement
- Diff – measured period
- AvgDiff – running average

Torsional Constant κ

- Average period **T = 43.45**[s]
- Moment of inertia **I ≈ 0.0355**[kg·m^2]

$$\mathbf{T} = 2\pi\sqrt{\frac{\boldsymbol{I}}{\boldsymbol{\kappa}}}$$

$$\boldsymbol{\kappa} = \frac{4\pi^2 I}{T^2} \approx \mathbf{7.42 \times 10^{-4}}\text{[Nm/rad]}$$

© 2026 Mikolaj Baczynski mikolaj.bzk@gmail.com

Calculating the Twisting Force

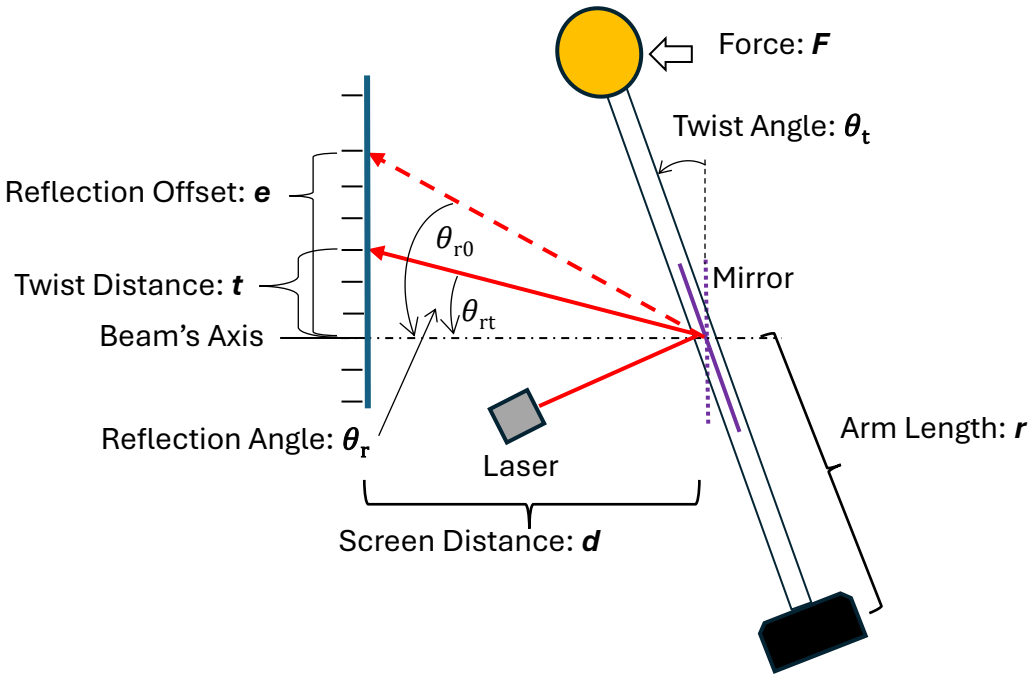

Calculating the Twist Angle: θ_t

- at $\theta_t = 0$: $\theta_{r0} = Atan\left(\frac{\text{Reflection Offset: e}}{\text{Screen Distance: d}}\right)$
- at Twist Distance t: $\theta_{rt} = Atan\left(\frac{\text{Twist Distance: t}}{\text{Screen Distance: d}}\right)$

Twist Angle:

- $\theta_t = 0.5 \cdot (\theta_{r0} - \theta_{rt})$

Calculating the Force: F

- total torque: $\tau = \kappa\theta_t$
- Force: $F = \frac{\tau}{r}$; for Dual Magnet configuration $F = \frac{\tau}{2r}$

Sign Convention:

- Angles are measured counterclockwise
- Forces are measured left-to-right

© 2026 Mikolaj Baczynski mikolaj.bzk@gmail.com

Analysis of Test configurations

How the interactions with the Earth's magnetic field affect tests' ability to reliably detect the Quantum Force (QF).

The following options were analyzed and tested:

- Dual Magnet Cancelling
- Dual Magnet Non-Cancelling
- Single Magnet
  - Mu-metal shielding
  - NS vs SN orientation of the Base Magnets

Only Single Magnet option is presented in this paper. Dual Magnet options turned out to be not reliable.

README.txt on google drive points to the documents describing all types of tests in detail:
https://drive.google.com/drive/folders/1kyX9nqq-aMQAfwHtXjgVs02RM9rtdCLb?usp=drive_link

© 2026 Mikolaj Baczynski mikolaj.bzk@gmail.com

Testing with Single Magnet Configurations

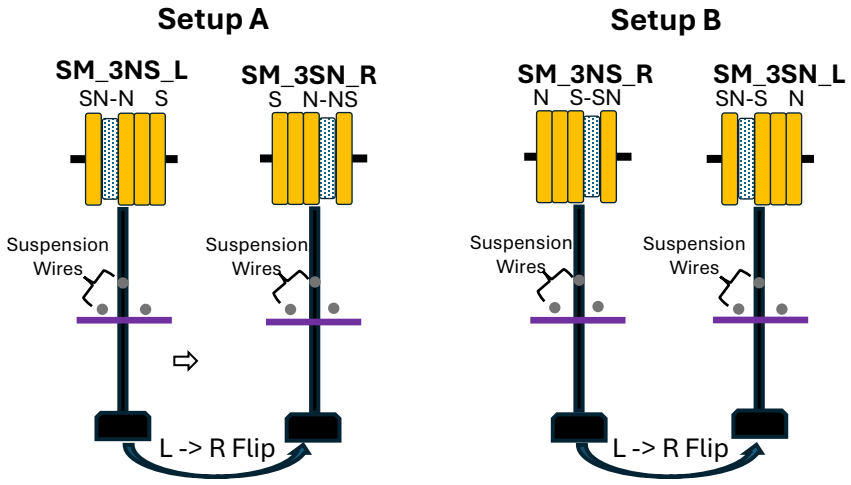

Note:

- 2 physical assemblies**: NS_L and NS_R**
- Flipping changes them to **SN_R** and **SN_L**

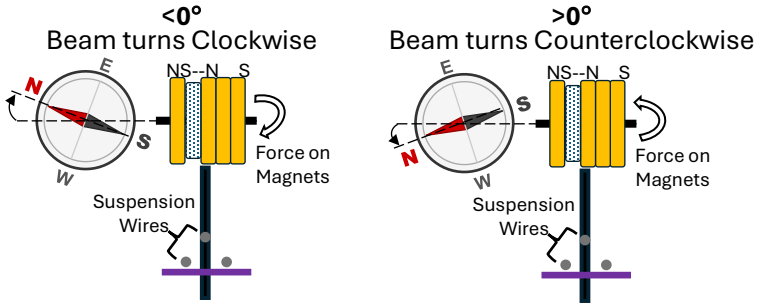

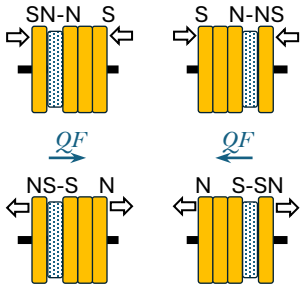

For a single N55 magnet, 29.4 mm diameter, 4,7mm thick, given Earth's B_h of 17.8μT and the compass angle of 2°, the Bias Force is:

- Theoretical: 6.55[μN]
- Measured: 5.77[μN]
- FEMM: 5.92[μN]

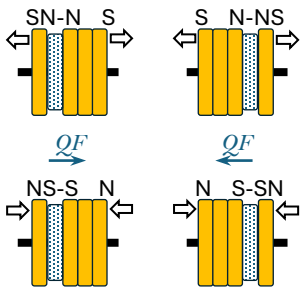

© 2026 Mikolaj Baczynski mikolaj.bzk@gmail.com

Force Analysis

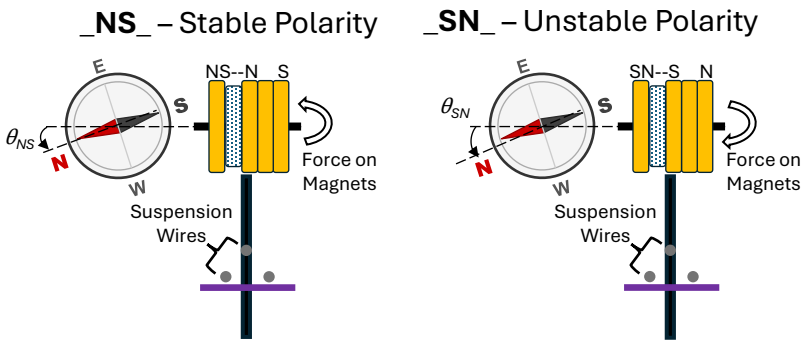

If the magnets are not perfectly shielded from the earth's magnetic filed, in the _QF configuration there exist a bias:

- **Positive,** where direction of the force due to the small magnet is the same as the expected Quantum Force
- **Negative,** where direction of the force due to the small magnet is the opposite as the expected Quantum Force

Note, the following Bias analysis is Only applicable in the pure dipole mode. Experiments show clearly that it Not the case; i.e. **the pictures below are just a simplified illustration**

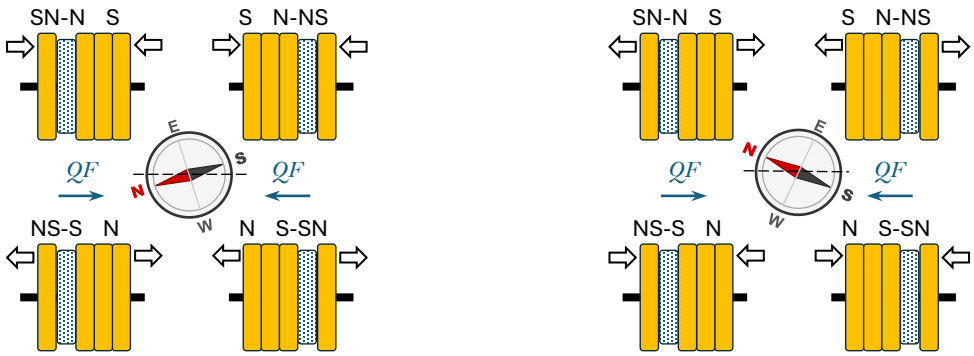

Small Angle:
The instability of the SN configuration (Base Magnets or Single Magnet) is not a clean Earth-coupling term; **it's nonlinear and can produce forces that may not follow sin(θ)**

© 2026 Mikolaj Baczynski mikolaj.bzk@gmail.com

Estimating the Force due to the Earth's magnetic field

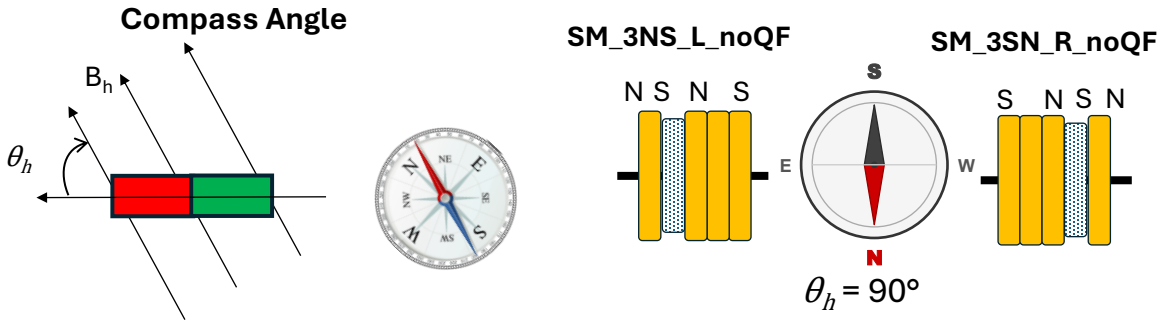

Given neodymium magnets: N55, 30mm diameter, 5mm thickness:

- magnetic moment of the single magnet: $\mathbf{m} = \frac{Br \cdot V}{\mu_0} \approx 4.219$ [A·m^2]
- $\mathbf{B_h}$ = 17.8 [μT]

we obtain:

- $\boldsymbol{\tau} = m \cdot B_h \cdot \sin(\theta_h) = 4.219 \cdot 17.8 \cdot 10^{-6} \cdot \sin(\theta_h)$[Nm]

Thus, force due to the single magnet

$$\mathbf{F} = \frac{\tau}{r} = \frac{75.1 \times 10-6}{0.4} \cdot \sin(\theta_h)$$

- at $\theta_h = 90°$, F = 187.75 [μN]; **750.98 [μN]** for the whole assembly
- at $\theta_h = 3°$, F = 9.82 [μN]
- at $\theta_h = 1°$, F = 3.27 [μN]

Configuration (**Assembly**)	torque: τ [Nm]	Force: F [N]	Measured Period: T [s]
NS			
SM_3NS_L_noQF	2.63E-04	**6.58E-04**	43.40
SM_3NS_R_noQF	2.69E-04	**6.71E-04**	43.40
3SN			
SM_3SN_L_noQF	-2.61E-04	**-6.53E-04**	43.40
SM_3SN_R_noQF	-2.50E-04	**-6.25E-04**	43.40

Test results report the force F between 671 [μN] and 625[μN].
≈15% from the calculated 751 [μN] is quite acceptable given the estimation of the magnetic moment, accuracy of B_h, and environmental noise.

© 2026 Mikolaj Baczynski mikolaj.bzk@gmail.com

Vertical Component of the Earth's magnetic field

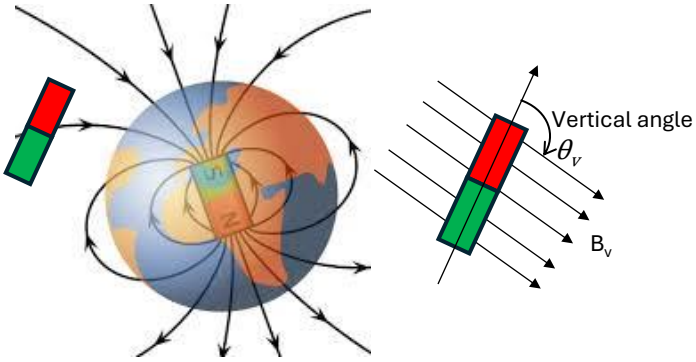

At the test location	
Total field, B_T	**55–56μT**
Horizontal component, B_h	**17–18μT**
Vertical component, B_v	**52–53μT downward**
Vertical component, B_v measured	**40.20μT** (median)**:** IQR 0.38
Inclination (dip angle), I	**≈71° downward**
Declination, D	**≈11° East** (magnetic north is east of true north)

Given neodymium magnets: N55, 30mm diameter, 5mm thickness:

- magnetic moment of the single magnet: $\mathbf{m} = \frac{Br \cdot V}{\mu_0} \approx 4.219$ [A·m^2]
- $\mathbf{B_v} = 53$ [μT]

we obtain:

- $\boldsymbol{\tau} = 4 \cdot m \cdot B_v = 4 \cdot 4.219 \cdot 53 \cdot 10^{-6} = 894.41 \cdot 10^{-6}$ [Nm]

Thus, given the assembly's length of ~25mm, force due to the single magnet

$\mathbf{F} = \frac{\tau}{0.0125} =$ **71.55**[mN]

1g of weight = **9.81**[mN]

Thus, the force due to the vertical component:

- Constant if, unless the assembly's position changes between tests
- Equivalent to 7.29[g] of weight: i.e. ~7% of the weight of the assembly (105.7[g])

The Vertical component of the Earth's magnetic field, B_v, contributes ~<7% to the effect due to the shift of the Magnet Assembly between tests: see Errors due to Assembly Placement

© 2026 Mikolaj Baczynski mikolaj.bzk@gmail.com

Estimating interaction with Earth's magnetic field using FEM

Earth's Field Not Included in the Model!

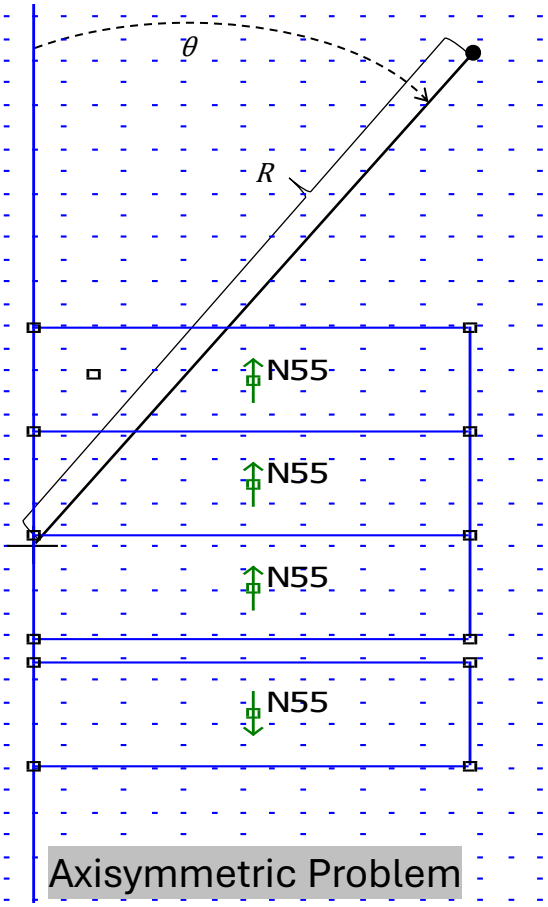

Three methods were compared:

Flux density $: \mathbf{T}_{Fm} = B_h \frac{4\pi R^3 \sqrt{B_r{}^2 + B_z{}^2}}{\mu_0 \sqrt{1+3cos^2\alpha}}$

Magnetic Moment $: \mathbf{T}_m \approx B_h \frac{2\pi R^3}{\mu_0} \sum_{i=0}^{N} B_{\text{rad}}(\theta_i) \cos(\theta_i) \sin(\theta_i)\ \Delta\theta$

Maxwell Tensor $: \mathbf{T}_g = \oint_S \boldsymbol{r} \times (\boldsymbol{T}_{\text{cross}} \cdot \boldsymbol{n})\, dS$

Then $F = \frac{\boldsymbol{T}}{r_{\text{arm}}}$

Method resulting in the best convergence vs R should be chosen.

Force at the Compass Angle of 90°:

- Calculated: 751[μN]
- FEMM: ~**680**[μN]
- Measured: ~**658**[μN]

Note: FEMM prediction m·Bh/r = 684[μN] (nominal field, 17.8[μT]); at the locally measured field (17.11[μT]) this is 657[μN], matching the measured 658[μN].

© 2026 Mikolaj Baczynski mikolaj.bzk@gmail.com

FEM: comparison of methods

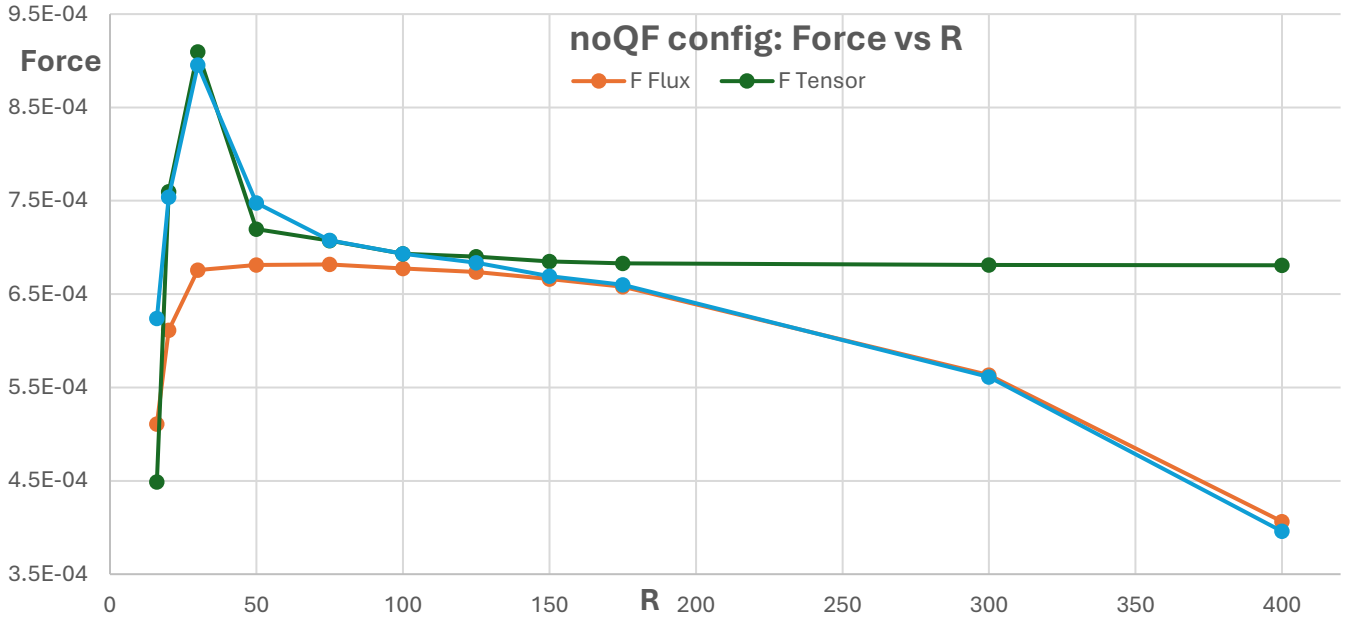

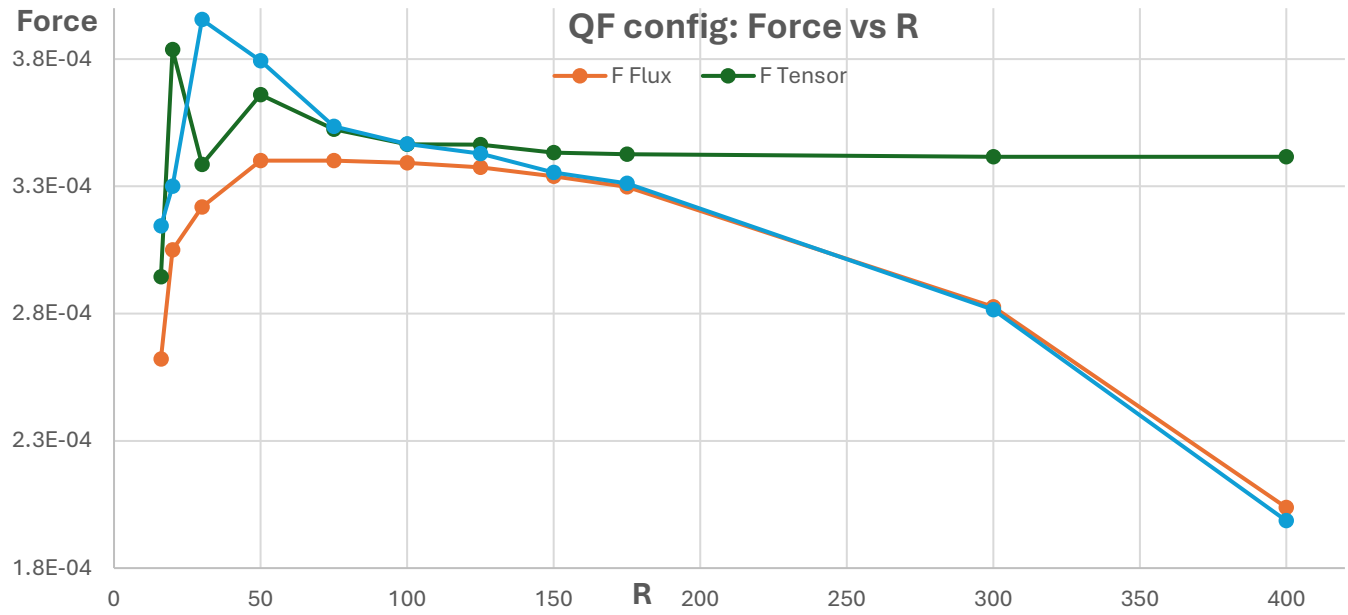

The Tensor (Maxwell-stress surface integral) method provides the best convergence

R	16	20	30	50	75	100	125	150	175	300	400
QF/noQF	0.6557	0.5049	0.3723	0.5087	0.4982	0.4999	0.5019	0.5012	0.5015	0.5015	0.5016

Note: The QF/noQF force ratio converges for R ≥ 50; the small-R values (0.66, 0.50, 0.37 at R = 16, 20, 30) are unconverged and are not used. The converged Tensor-method ratio is ≈0.502 (large-R asymptote 0.5016), consistent with the adopted FEMM moment ratio R = 0.5035 to within ~0.4%. R = 0.5035 (FEMM) is adopted throughout; the ~0.4% difference is the inter-method/mesh spread**.**

© 2026 Mikolaj Baczynski mikolaj.bzk@gmail.com

Estimating the Force due to environmental contamination

Given a piece of iron r distance away from the magnet assembly, the resulting force F can be estimated as follows:

$$F = \frac{3\,\mu_0\,\chi}{(4\pi)^2} \cdot \frac{M}{\rho} \cdot \frac{m^2}{r^7}$$

where:

- $\mu_0 = 4\pi \times 10^{-7}$ T·m/A
- χ = magnetic susceptibility of iron (~200 for mild steel, up to 1000 for soft iron)
- **M** = mass of iron piece in kg
- **ρ** = 7874 kg/m^3 (iron density)
- **m** = assembly's dipole moment in A·m^2
- **r** = distance in metres

With the dipole moment of the assembly, m = 15.25 A·m^2, and mild steel (χ=200), we obtain the following table:

Mass	r = 0.5m	r = 1.0m	r = 1.2m
	F [nN]	F [nN]	F [nN]
1g	18.1	0.14	0.04
10g	180.5	1.41	0.39
50g	902.5	7.05	1.97
100g	1805	14.1	3.94
200g	3610	28.2	7.87
500g	9025	70.5	19.7
1kg	18051	141	**39.4**

© 2026 Mikolaj Baczynski mikolaj.bzk@gmail.com

Errors due to Assembly Placement

Tested 5mm shifts to the right (5mmR = clockwise direction) and left (5mmL = counter-clockwise).
Moving the assembly along the beam is no issue i.e. it is secured with accuracy better than 0.2mm. Given the beam's length of 400mm, that results in the maximum jitter below 0.1%.

Extracted Force Changes (ΔF relative to nominal "0")

Configuration	Shift	ΔF for 5 mm [μN]	Sensitivity [μN / mm]	Expected ΔF at 0.1 mm [μN]
L_QF	5 mm R	+6.3	1.27	0.13
	5 mm L	–10.4	2.08	0.21
R_QF	5 mm R	–1.0	0.20	0.02
	5 mm L	–14.0	2.81	0.28
noQF	5 mm R	+4.4	0.88	0.09
	5 mm L	–9.5	1.88	0.19

Note: the construction of the assembly holder ensured placement accuracy of ±0.1mm.

© 2026 Mikolaj Baczynski mikolaj.bzk@gmail.com

Open-ended, Shielded Configuration

Two-layer cylindrical mu-metal shielding

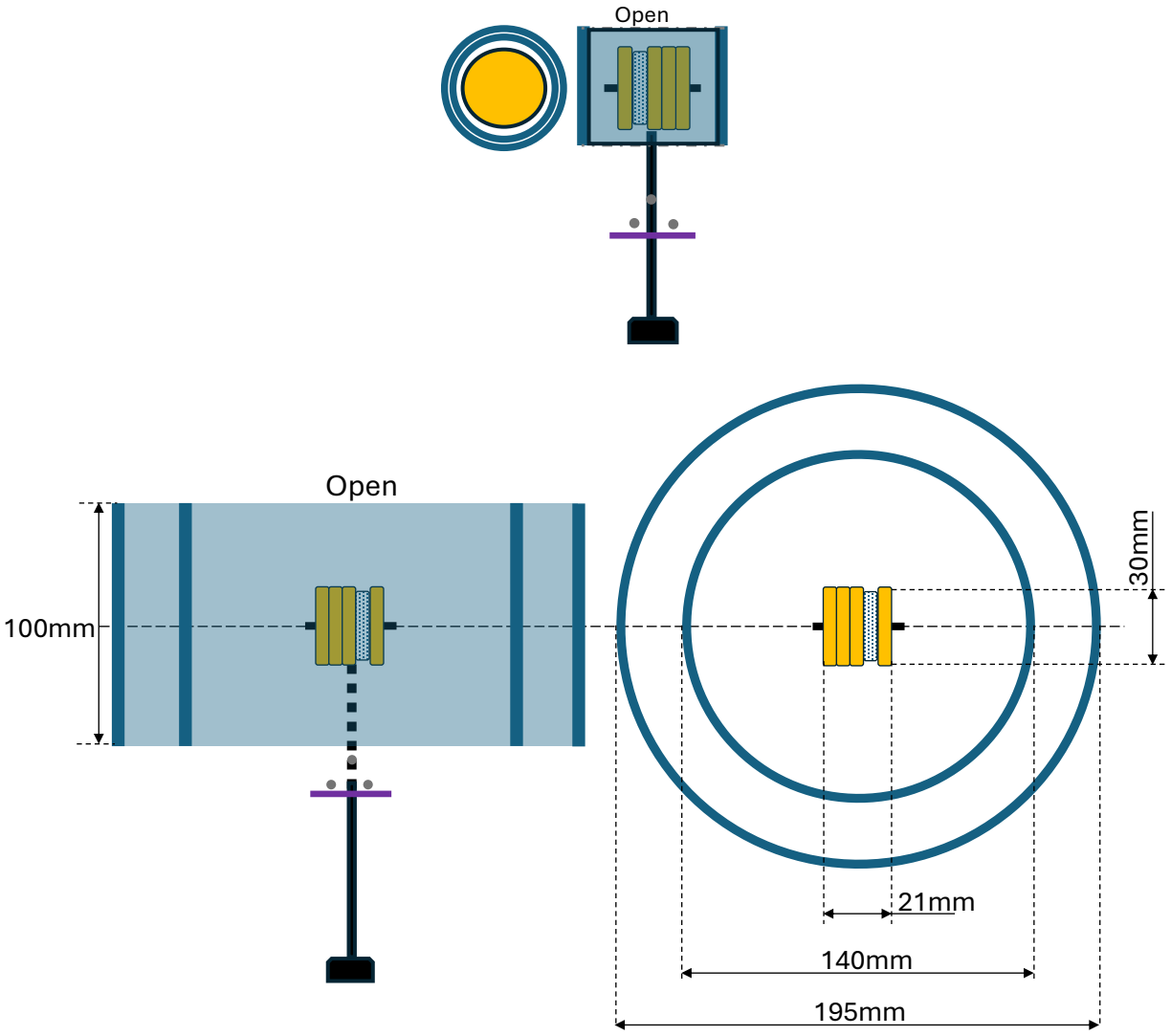

© 2026 Mikolaj Baczynski mikolaj.bzk@gmail.com

Mu-metal, Shunting Not Shielding

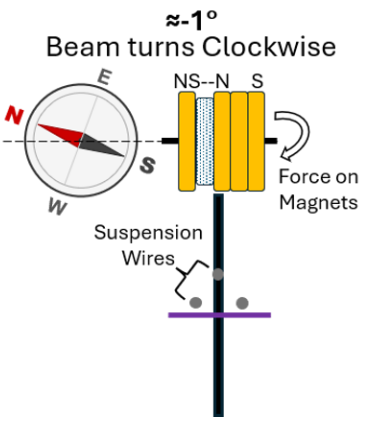

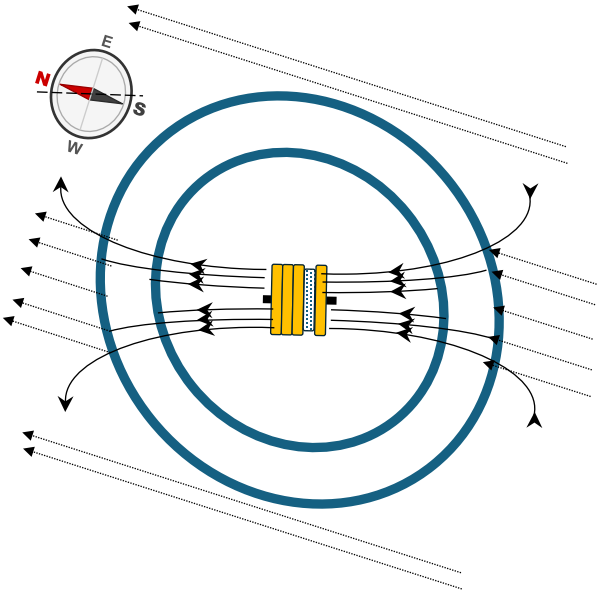

Configuration (Assembly)	Twist Angle in Degrees	Force: F [N]
_3NS_		
SM_3NS_L_noQF (A)	-0.19	1.18E-05
SM_3NS_R_noQF (B)	-0.65	4.14E-05
Mu-metal Shielded		
SM_3NS_L_noQF (A)	-0.09	8.71E-06
SM_3NS_R_noQF (B)	-0.14	1.31E-05
_3SN_		
SM_3SN_L_noQF (B)	-0.14	**8.82E-06**
SM_3SN_R_noQF (A)	-0.28	1.77E-05
Mu-metal Shielded		
SM_3SN_L_noQF (B)	-0.23	**2.18E-05**
SM_3SN_R_noQF (A)	-0.18	1.74E-05

Comparing the force for the Shielded and Un-shielded configurations we see that for the NS orientation of the assemblies there is a significant **decrease** of the force due to the interaction with the Earth's field. However, for the SN orientation there is even a significant **increase** (8.82E-06vs 2.18E-05).

This is a very clear indication of flux shunting through the nearby mu-metal.

© 2026 Mikolaj Baczynski mikolaj.bzk@gmail.com

Estimating QF Based on Test Results

Method A. Using FEM's effective moment's ratios:

- $R = \frac{m_{eff_QF}}{m_{eff_noQF}}$
- F_{noQF} – force measured in _noQF configuration
- F_{QF} – force measured in _QF configuration

  Then if $|F_{QF}| > |R \cdot F_{noQF}|$ then,
- $|\boldsymbol{QF}| = |F_{QF}| - |R \cdot F_{noQF}|$

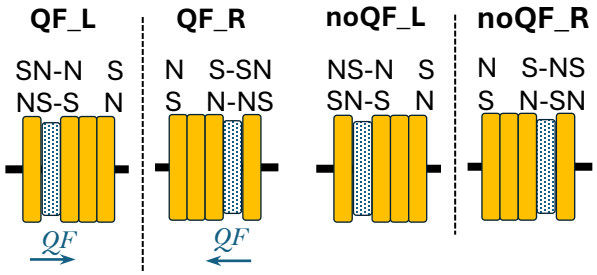

Method B. Comparing forces in _R and _L _QF configuration tests:

- F_{BM} – force due to the Base Magnets
- F_{SM} – force due to the Single Magnet
- F_{QF} – the Quantum Force

If we subtract _L forces from _R forces, we get

- **QF = 0.5*(F_R – F_L)**

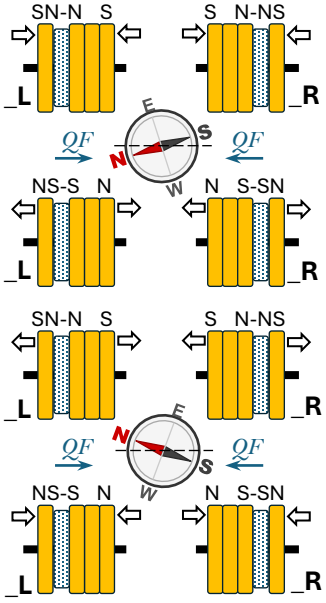

Method C. Comparing Results from different Compass Angles:

- θ_1, θ_2 – **Compass Angles; inferred from F_{noQF}**
- F_1, F_2 - _QF forces obtained for θ_1 and θ_2

Assuming $F = C \cdot \sin(\theta) + QF$

- $\boldsymbol{QF} = \frac{F_1 \sin(\theta_2) - F_2 \sin(\theta_1)}{\sin(\theta_2) - \sin(\theta_1)}$
- $C = \frac{F_1 - F_2}{\sin(\theta_1) - \sin(\theta_2)}$

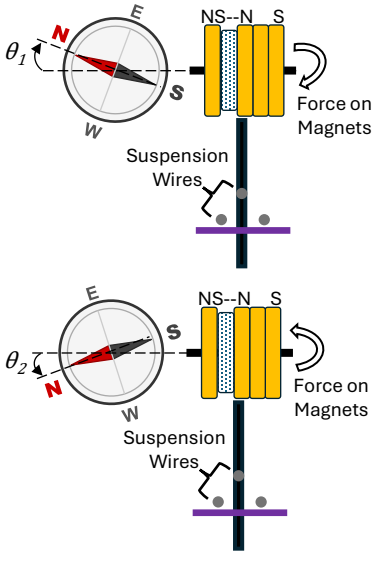

© 2026 Mikolaj Baczynski mikolaj.bzk@gmail.com

Comparison of QF Detection Methods

Method A. Using FEM's effective moment's ratios:

- $R = \frac{m_{eff_QF}}{m_{eff_noQF}}$

  Then if $|F_{QF}| > |R \cdot F_{noQF}|$ then,
- $|\boldsymbol{QF}| = |F_{QF}| - |R \cdot F_{noQF}|$

Method B. Comparing forces in _R and _L _QF configurations tests:

- $\mathbf{QF = 0.5*(F_R - F_L)}$

Method C. Comparing Results from different Compass Angles ($F = C \cdot \sin(\theta) + QF$):

- $\mathbf{QF} = \frac{F_1 \sin(\theta_2) - F_2 \sin(\theta_1)}{\sin(\theta_2) - \sin(\theta_1)}$

Assumption	Method B	Method C	Method A
1. FEMM torque accurate	no	no	YES
2. m_{eff} ratio R correct	no	no	YES
3. Force ∝ sin θ	no	YES	partial
4. Assembly = one dipole	weak	YES	YES
5. C constant across paired angles	n/a	YES	no
6. L/R symmetry |F_L|=|F_R|	YES	no	no
7. Single magnet pinned (not wandering)	YES	YES	YES

Method B - **relies on the fewest number of Assumptions!**

- L/R asymmetry must be considered for both QF and noQF configurations, i.e.:

$$QF = 0.5*[(F_{R_QF} - F_{L_QF}) - (F_{R_noQF} - F_{L_noQF})]$$

Method C - **does not consider the single magnet's bias**

- only applicable to Negative Bias configurations
- QF may be undetectable if the Bias force too high

Method A - **cannot be used; it requires magnets to act as perfect dipoles**

- small angle SN magnets result in unclean Earth-coupling term that is nonlinear and can produce forces that do not follow sin(θ)
- Method A may be used if the Earth's field is nulled or $F_{_noQF}$ small and no SN instability

© 2026 Mikolaj Baczynski mikolaj.bzk@gmail.com

Beam Calibration Results

Comparing measured, _noQF forces, F_meas, with predicted, F_pred,

- Given FEMM magnetic moment of 15.36[A·m^2]
- Given location's B_h from Environment Canada of 17.80[μT]
- Given location's B_h measured by BMM150 magnetometer of 17.11[μT]

Note:

- the Compass (E-W) Angle, θ, is itself inferred from the measured noQF force and the reference amplitude, cell A63 (658[μN]), (θ = arcsin(−F_noQF / A63))
- independent check comes the measured field (17.1[μT]) combined with the FEM moment (15.36 A·m^2) that results in 657[μN], reproducing the measured maximum force from A63 withing 0.15%

Run	Config	twist θ_t [°]	E-W θ [°]	sinθ	F_meas [μN]	F_pred @17.8 [μN]	F_pred @17.11 [μN]	resid @17.11	ratio
Run2	NS_L	0.479	1.596	0.0278	-18.32	-19.03	-18.30	-0.03	1.002
	NS_R	0.446	1.485	0.0259	-17.06	-17.72	-17.03	-0.03	1.001
	SN_L	-0.782	-2.602	-0.0454	29.88	31.04	29.83	0.04	1.002
	SN_R	-0.879	-2.927	-0.0511	33.60	34.91	33.55	0.05	1.001
Run3	NS_L	0.227	0.756	0.0132	-8.68	-9.01	-8.66	-0.01	1.001
	NS_R	0.181	0.603	0.0105	-6.92	-7.19	-6.91	-0.01	1.001
	SN_L	-0.435	-1.447	-0.0253	16.62	17.26	16.59	0.02	1.001
	SN_R	-0.530	-1.765	-0.0308	20.27	21.06	20.24	0.03	1.001
Run4	NS_L	0.055	0.199	0.0035	-2.29	-2.38	-2.28	0.00	1.001
	NS_R	-0.028	-0.100	-0.0017	1.14	1.19	1.14	0.00	1.001
	SN_L	-0.017	-0.062	-0.0011	0.71	0.74	0.71	0.00	1.002
	SN_R	-0.134	-0.482	-0.0084	5.54	5.75	5.53	0.01	1.002
Run5	NS_L	-0.340	-1.189	-0.0207	13.65	14.18	13.63	0.02	1.002
	NS_R	-0.350	-1.225	-0.0214	14.06	14.61	14.04	0.02	1.001
	SN_L	0.156	0.547	0.0095	-6.28	-6.53	-6.27	-0.01	1.002
	SN_R	0.133	0.466	0.0081	-5.35	-5.56	-5.34	-0.01	1.001
Run6	NS_L	-0.596	-2.088	-0.0364	23.97	24.90	23.94	0.04	1.001
	NS_R	-0.673	-2.356	-0.0411	27.05	28.09	27.01	0.04	1.002
	SN_L	0.653	2.287	0.0399	-26.25	-27.27	-26.22	-0.04	1.001
	SN_R	0.544	1.905	0.0332	-21.87	-22.72	-21.84	-0.03	1.001
Run7	NS_L	-0.578	-2.002	-0.0349	22.98	23.87	22.95	0.03	1.001
	NS_R	-0.687	-2.381	-0.0415	27.33	28.39	27.29	0.04	1.001
	SN_L	0.854	2.961	0.0516	-33.98	-35.30	-33.93	-0.05	1.001
	SN_R	0.681	2.359	0.0412	-27.09	-28.14	-27.05	-0.04	1.001
Run8	NS_L	-0.777	-2.722	-0.0475	31.25	32.46	31.20	0.05	1.001
	NS_R	-0.777	-2.722	-0.0475	31.25	32.46	31.20	0.05	1.001
	SN_L	0.978	3.426	0.0598	-39.32	-40.84	-39.26	-0.06	1.001
	SN_R	0.808	2.830	0.0494	-32.49	-33.75	-32.44	-0.05	1.001

© 2026 Mikolaj Baczynski mikolaj.bzk@gmail.com

Main Test Results, Method C

The E-W (compass) angle is inferred from $F_{_noQF}$, thus, the following are consequences of that construction, not independent measurements:

- the value of QF for the noQF configurations < **10E-21**[N]
- the slope "C" in F = C·sin(θ) + QF is common to all noQF runs. These confirm the internal consistency of the data reduction; **they are not evidence that the apparatus is free of a mechanical offset**. The one check that does not use the inferred angle is the amplitude: the noQF slope C ≈ 658[μN] agrees with $m \cdot B_h/r$ from the FEM-modelled moment and the separately measured horizontal field.

- **Caution:** Run7 NS shows ~same E-W angle as Run6 despite ~2° beam twist

Run4 looks coherent against ALL runs; because near θ ≈ 0° Method C is just reading the raw force: i.e. **the 'noise' comes mainly from one angle, not two**. SN_R is the least stable.

	NS_L			NS_R			SN_L			SN_R	
Sheet	E-W: θ[°]	Method C QF[N]		E-W: θ[°]	Method C QF[N]		E-W: θ[°]	Method C QF[N]		E-W: θ[°]	Method C QF[N]
Run1	2.6			2.6			-3.9			-3.9	
Run2	1.6	5.68E-06		1.5	-2.96E-06	vs Run1	-2.6	5.16E-06		-2.9	-9.29E-06
Run3	0.8	3.11E-06		0.6	-4.29E-07	vs Run2	-1.4	3.08E-06		-1.8	-3.51E-07
		3.78E-06			-1.01E-06	vs Run1		3.70E-06			-2.84E-06
Run4	0.2	5.20E-06		-0.1	-3.60E-06	vs Run3	-0.1	2.13E-06		-0.5	-5.55E-06
		4.87E-06			-3.90E-06	vs Run2		2.15E-06			-4.88E-06
		4.91E-06			-3.92E-06	vs Run1		2.18E-06			-5.09E-06
Run5	-1.2	4.70E-06		-1.2	-4.85E-06	vs Run4	0.5	1.87E-06		0.5	-1.16E-06
		3.84E-06			1.04E-06	vs Run3		2.47E-07			1.28E-06
		4.18E-06			2.02E-06	vs Run2		-1.45E-07			1.43E-06
		3.88E-06			3.23E-06	vs Run1		-4.75E-07			1.82E-06
Run6	-2.1	5.70E-06		-2.4	8.11E-06	vs Run5	2.3	-2.32E-06		1.9	1.62E-06
		4.63E-06			-4.32E-06	vs Run4		2.22E-06			-2.89E-06
		3.46E-06			-2.85E-07	vs Run3		3.42E-06			7.71E-07
		3.68E-06			-1.55E-07	vs Run2		3.54E-06			1.06E-06
		3.11E-06			8.57E-07	vs Run1		3.24E-06			2.22E-06
Run7	-2.0	3.00E-05		-2.4	2.18E-04	vs Run6	3.0	1.55E-06		2.4	2.63E-05
		4.23E-06			1.05E-05	vs Run5		-2.07E-06			3.08E-06
		4.73E-06			-4.22E-06	vs Run4		2.23E-06			-4.08E-06
		3.76E-06			-7.49E-07	vs Run3		3.60E-06			-1.84E-06
		4.16E-06			-1.04E-06	vs Run2		3.82E-06			-2.28E-06
		3.74E-06			-3.39E-07	vs Run1		3.52E-06			-1.38E-06
Run8	-2.7	3.04E-06		-2.7	-2.63E-06	vs Run7	3.4	1.48E-05		2.8	-5.80E-06
		-1.94E-06			1.44E-05	vs Run6		5.74E-06			1.32E-05
		3.90E-06			8.92E-06	vs Run5		-1.56E-06			2.73E-06
		4.77E-06			-4.21E-06	vs Run4		2.19E-06			-4.03E-06
		3.82E-06			-7.00E-07	vs Run3		3.07E-06			-1.54E-06
		4.31E-06			-9.56E-07	vs Run2		3.07E-06			-1.92E-06
		3.87E-06			-1.77E-07	vs Run1		2.58E-06			-8.70E-07

© 2026 Mikolaj Baczynski mikolaj.bzk@gmail.com

Main Test Results, Method B

The Fewest Assumptions

	NS_L	NS_R	H	K	QF_B		SN_L	SN_R	H	K	QF_B
Sheet	E-W: θ[°]	E-W: θ[°]	QF = 0.5(F_R-F_L)	noQF 0.5(F_R-F_L)	**0.5(F_R-F_L) QF - noQF**		E-W: θ[°]	E-W: θ[°]	QF = 0.5(F_R-F_L)	noQF 0.5(F_R-F_L)	**0.5(F_R-F_L) QF - noQF**
Run1	2.6	2.6	-1.1E-06				-3.9	-3.9	-1.20E-06		
Run2	1.6	1.5	-2.13E-06	6.34E-07	**-2.77E-06**		-2.6	-2.9	-1.83E-06	1.86E-06	**-3.69E-06**
Run3	0.8	0.6	-1.62E-06	8.78E-07	**-2.50E-06**		-1.4	-1.8	-1.39E-06	1.83E-06	**-3.22E-06**
Run4	0.2	-0.1	-3.5E-06	1.72E-06	**-5.25E-06**		-0.1	-0.5	-2.00E-06	2.41E-06	**-4.41E-06**
Run5	-1.2	-1.2	1.73E-07	2.07E-07	**-3.46E-08**		0.5	0.5	1.71E-06	4.66E-07	**1.24E-06**
Run6	-2.1	-2.4	-3.1E-07	1.54E-06	**-1.84E-06**		2.3	1.9	9.82E-07	2.19E-06	**-1.21E-06**
Run7	-2.0	-2.4	-1.7E-06	2.17E-06	**-3.84E-06**		3.0	2.4	-1.40E-06	3.45E-06	**-4.85E-06**
Run8	-2.7	-2.7	-2.93E-06	0.00E+00	**-2.93E-06**		3.4	2.8	-2.42E-07	3.42E-06	**-3.66E-06**

- **If QF exists**: QF-config's F_R-F_L = (2·QF) + (L/R asymmetry), while noQF's F_R-F_L = (L/R asymmetry alone). Subtracting them, (QF−noQF), removes the asymmetry and leaves 2·QF. The possible error comes from the fact L/R asymmetries for QF and noQF configurations re not the same.
- **If QF does not exist**: QF's F_R-F_L = (L/R asymmetry), and noQF's F_R-F_L = (L/R asymmetry). Both are just asymmetries; however, their values are different and **QF – noQF ≠ 0**.

Those asymmetries are polarity-dependent classical Earth coupling, they scale with sin(θ)

Expectation for Method B is that all QF_B values are that same and their sign in negative, i.e. consistent with the expected direction of the QF force; H and K based on (F_R-F_L)

Result: persistent negative residual, not reproducible in magnitude.

Every run is ≤ 0 (six clearly negative, Run 5 ≈ 0), but the magnitude varies ~3× (−1.8 to −5.3 μN) and the cleanest-baseline runs disagree (Run 8, |K| = 0.00: −2.9 μN; Run 5, |K| = 0.21: ≈ 0). The |K_NS| ≤ 0.9 μN filter uses noQF readings alone and was adopted during analysis. It shares data with the residual QF_B = H − K, so statistical independence from that residual cannot be assumed. See the table below.

Selection	runs	n	QF_B(NS) [μN]	95% CI → interval
All complete runs	2–8	7	−2.7	±1.5 → [−4.2, −1.2]
Baseline-qualified: |K_NS| ≤ 0.9 μN	**2, 3, 5, 8**	**4**	**−2.1**	**±2.2 → [−4.2, +0.1]**
Baseline-qualified without Run5	2, 3, 8	3	−2.7	±0.5 → [−3.3, −2.2]
Run 2 & Run 8 (original design)	2, 8	2	−2.85	±1.1 → [−3.9, −1.8] (CI dominated by t, not precision)

© 2026 Mikolaj Baczynski mikolaj.bzk@gmail.com

Main Test Results, Method A
Run 4 Results

Too much instability!

Configuration (Assembly)	Twist Angle: θ_t [°]	Force: F [N]	QF = F_{QF}-(R*F_{noQF})
Median Based			
_NS_			
NS_L_noQF	0.06	-2.29E-06	
NS_L_QF	-0.09	3.57E-06	4.72E-06
NS_R_noQF	-0.03	1.14E-06	
NS_R_QF	0.08	-3.50E-06	-4.08E-06
_SN_			
SN_R_noQF	-0.13	5.54E-06	
SN_R_QF	0.03	-1.43E-06	-4.22E-06
SN_L_noQF	-0.02	7.15E-07	
SN_L_QF	-0.06	2.57E-06	2.21E-06

- **Event though F_noQF is small there is a lot of L/R asymmetry**
- **Consistent direction of QF, however SN_L_QF value is out of range**

© 2026 Mikolaj Baczynski mikolaj.bzk@gmail.com

Test Run Variations

Note: the Twits Distance, ***t***, includes ± 0.5mm uncertainty in reading the beam position.
Note: the STD and IQR rows are relative dispersions — population SD (and IQR) divided by |mean| of the nine readings. The uncertainty propagation instead uses the absolute sample SD (in metres).

The residual uncertainty is propagated as $u^2(R) = a^T \Sigma a$ with a = (1, −1, −1, 1)/2, retaining the shared-calibration (κ, r, gain) correlations across the four forces (details on google drive). The shared-calibration relative uncertainties (uκ/κ = 2 %, ur/r = 1 %, ug/g = 2 %) are illustrative inputs, not independently calibrated. The quoted run-to-run interval does not bound these shared systematics, nor the configuration-dependent coupling, which remains unbounded.

	Test # Twist Distance: t [m]	NS_L_noQF	NS_L_QF	NS_R_noQF	NS_R_QF	SN_R_noQF	SN_R_QF	SN_L_noQF	SN_L_QF
Run1	Median	0.4390	0.4655		0.4620	0.5553	0.5233		0.5270
	Mean(Average)	0.4379	0.4651		0.4619	0.5541	0.5232		0.5270
	IQR	**0.456%**	**0.269%**		**0.162%**	**1.441%**	**0.182%**		**0.285%**
	STD	**0.343%**	**0.241%**		**0.134%**	**0.707%**	**0.132%**		**0.154%**
Run2	Median	0.3335	0.3538	0.3355	0.3470	0.4163	0.3881	0.4103	0.3939
	Mean(Average)	0.3333	0.3538	0.3357	0.3471	0.4167	0.3882	0.4103	0.3939
	IQR	**0.075%**	**0.353%**	**0.447%**	**0.403%**	**0.240%**	**0.129%**	**0.609%**	**0.127%**
	STD	**0.194%**	**0.253%**	**0.360%**	**0.426%**	**0.303%**	**0.241%**	**0.326%**	**0.102%**
Run3	Median	0.1967	0.2085	0.1994	0.2035	0.2413	0.2247	0.2357	0.2290
	Mean(Average)	0.1965	0.2085	0.1993	0.2036	0.2417	0.2249	0.2365	0.2290
	IQR	**0.509%**	**0.360%**	**0.752%**	**0.369%**	**0.705%**	**0.334%**	**1.379%**	**0.437%**
	STD	**0.427%**	**0.269%**	**0.490%**	**0.333%**	**0.424%**	**0.333%**	**0.664%**	**0.318%**
Run4	Median	0.0548	0.0630	0.0596	0.0531	0.0658	0.0560	0.0590	0.0616
	Mean(Average)	0.0548	0.0630	0.0595	0.0533	0.0658	0.0563	0.0585	0.0618
	IQR	**1.369%**	**1.667%**	**1.342%**	**1.130%**	**1.749%**	**0.536%**	**10.339%**	**0.812%**
	STD	**1.139%**	**1.113%**	**0.950%**	**1.066%**	**1.181%**	**1.011%**	**5.926%**	**0.831%**
Run5	Median	-0.0933	-0.0965	-0.0927	-0.0960	-0.1208	-0.1143	-0.1221	-0.1193
	Mean(Average)	-0.0937	-0.0963	-0.0928	-0.0962	-0.1205	-0.1141	-0.1220	-0.1206
	IQR	**1.877%**	**1.347%**	**0.648%**	**1.562%**	**0.621%**	**1.094%**	**1.024%**	**2.725%**
	STD	**1.346%**	**0.793%**	**0.585%**	**1.001%**	**0.682%**	**0.704%**	**0.685%**	**1.627%**
Run6	Median	-0.2095	-0.2216	-0.2050	-0.2225	-0.2770	-0.2575	-0.2835	-0.2604
	Mean(Average)	-0.2094	-0.2218	-0.2045	-0.2225	-0.2769	-0.2578	-0.2838	-0.2606
	IQR	**0.597%**	**0.564%**	**0.537%**	**0.225%**	**0.325%**	**0.447%**	**0.705%**	**0.288%**
	STD	**0.458%**	**0.372%**	**0.418%**	**0.259%**	**0.260%**	**0.208%**	**0.369%**	**0.290%**
Run7	Median	-0.2745	-0.2845	-0.2680	-0.2895	-0.3500	-0.3348	-0.3605	-0.3305
	Mean(Average)	-0.2747	-0.2845	-0.2678	-0.2895	-0.3506	-0.3348	-0.3603	-0.3305
	IQR	**0.182%**	**0.176%**	**0.560%**	**0.518%**	**0.371%**	**0.149%**	**0.208%**	**0.303%**
	STD	**0.191%**	**0.125%**	**0.235%**	**0.306%**	**0.338%**	**0.182%**	**0.266%**	**0.202%**
Run8	Median	0.1343	0.1195	0.1343	0.1110	0.0421	0.0612	0.0323	0.0619
	Mean(Average)	0.1342	0.1195	0.1342	0.1110	0.0418	0.0611	0.0323	0.0620
	IQR	**0.372%**	**0.418%**	**0.074%**	**0.450%**	**1.781%**	**1.063%**	**1.550%**	**0.647%**
	STD	**0.270%**	**0.351%**	**0.125%**	**0.337%**	**1.445%**	**0.635%**	**1.290%**	**0.686%**

Quantity	Value
reading resolution	±0.32 μN / reading
reading scatter σ_t	sample SD: 0.179–1.569 mm for the 16 selected NS channel/run combinations
within-run $u(R) = \sqrt{(a^T \Sigma a)}$	0.32, 0.24, 0.28, 0.14 μN (Runs 2, 3, 5, 8) — median estimator; Run 5 ≈ 0.28 μN is a clean near-null, not a noisy run
run-to-run SD	1.36 μN
run-to-run 95% CI (quoted)	±2.2 μN

© 2026 Mikolaj Baczynski mikolaj.bzk@gmail.com

Test Run Summary

Key findings:

- Method C and B rely on different assumptions, thus, the instability due to SN magnets shows-up at different angles

Method B:

- The quoted uncertainty is the run-to-run 95% confidence interval (±2.2 μN), which covers reading noise within-run u(R) = 0.14–0.32 μN across runs (median estimator; SE_median ≈ 1.2533·s/√9, an approximate Gaussian-median standard error assuming independent readings), propagated as $u^2(R) = a^T \Sigma a$) and random run-to-run variation (SD ≈ 1.36 μN); it does not bound the common calibration bias (κ, r, gain; ~3%, an illustrative input that shifts every run together) nor the configuration-dependent coupling — the residual scales with the baseline asymmetry K (clean-baseline runs −2.1 μN vs baseline-contaminated −3.6 μN), a potential bias rather than a random error, and the dominant unresolved uncertainty. Part of the association with K can arise because K is subtracted in forming the residual; the association alone does not identify configuration-dependent contamination.

Method C: provides one independent check of the force scale plus several internal-consistency checks. Because the compass angle θ is inferred from F_noQF, the vanishing noQF intercept (R^2 = 1.00) and the QF/noQF slope ratio of 0.53 (matching the FEMM moment ratio R = 0.5035) follow from the data reduction — they confirm internal consistency, not an independently verified absence of a mechanical offset. The one genuinely independent quantity is the amplitude: the fitted noQF slope (658 μN) equals the separately measured maximum force (658 μN) and matches m·Bh/r = 657 μN at the measured field (684 μN at the nominal 17.8 μT) — a limited external-field/modeled-moment consistency check of the force scale, not a complete validation.

Near θ ≈ 0° (Run 4, |θ| ≤ 0.5°) the classical term vanishes and Method C reduces to the directly measured force with the partner run contributing negligibly ($\partial QF_C/\partial F_2 \to 0$), making Run-4-anchored estimates the most stable; the least stable input throughout is the SN configuration.

Discrepancy between Method B and C: The QF-configuration single-channel NS intercepts are +4.10 μN (NS_L) and −0.69 μN (NS_R). Their symmetric half-sum is the common-mode, +1.71 μN, and their antisymmetric half-difference is −2.39 μN; the large single-channel value (≈4 μN for NS_L) combines the two. The primary antisymmetric estimate is a different estimator: a single regression of the per-run antisymmetric force ½(F_R − F_L) on the mean R/L sin θ (7 runs, 5 residual dof, SE includes the R/L channel covariance) gives −1.87 ± 1.58 μN for NS (and −0.75 ± 1.44 μN for SN). This regression treats sin θ as exact, but θ is inferred from uncertain noQF readings, so the ordinary-regression scatter is a conditional regression uncertainty that omits predictor uncertainty, not its full value. Both the single-regression value (−1.87 ± 1.58 μN) and the channel-intercept antisymmetric value (−2.39 μN) agree, within uncertainty, with the primary Method-B result, −2.06 ± 2.17 μN. The apparent Method-B/Method-C disagreement is the +1.71 μN common-mode term that Method B removes by construction, not a genuine inconsistency

© 2026 Mikolaj Baczynski mikolaj.bzk@gmail.com

Conclusions

Experiments need to be repeated in a Shielded lab, or at least, with field nulling

Across seven runs the NS antisymmetric residual in the QF configuration is negative in six and near zero in the seventh (the qualifying null run), with a magnitude clustering at 2–3 μN and a sign consistent with the field geometry in the FEM model. It does not follow sin(θ). The predominantly negative sign pattern, with variable magnitude and a qualifying near-null run, is the central observation.

- The antisymmetric residual does not follow sin(θ) and is negative in six of seven runs (~2–3 μN) — reproducible in sign, not magnitude.
- Its sign matches the field geometry in the FEM model.
- The noQF configurations agree with dipole modelling in amplitude but carry a run-dependent left/right baseline asymmetry (K) that is only partially corrected.
- NS is the primary channel (less affected by SN instability); SN is corroborative at best.

The magnitude is not yet established: the baseline-qualified mean (Runs 2, 3, 5, 8) is −2.06 ± 2.17 μN ([−4.23, +0.11]). An exploratory subset excluding the near-null Run 5 (Runs 2, 3, 8) gives −2.73 ± 0.54 μN — sensitivity only, not the primary result. Methods B and C analyse the same data, so the agreement of the primary result with Method C's −1.87 ± 1.58 μN is an internal cross-check, not replication; the precise value is unresolved.

I'd like to emphasize the limits:

- In Earth's field the geometry-fixed and classical field-coupling terms are formally degenerate; the data constrain their sum near θ = 0 but cannot attribute it to a new force
- The SN configuration does not reconcile between the two methods (−0.7 $\pm$ 1.4 μN vs −3.5 μN) and carries a large, only partially corrected baseline asymmetry; NS is the primary result, SN corroborative at best
- The symmetric 1.7 μN common-mode in the QF configuration is not predicted by an antisymmetric QF and is an unexplained systematic
- The largest quantified random component is the run-to-run spread; configuration-dependent systematics remain unbounded

The reproducible few-μN antisymmetric residual is reported as a **configuration-dependent effect with unresolved systematics**, motivating a field-nulling measurement. It is a descriptive residual scale — not a detection of the Quantum Force, and not a rigorous upper bound

Highly Speculative:

- The vacuum energy required to support the results is on the order of 2.60E-09[J/m^3] i.e., it motivates a concrete question for future work — whether the _QF configuration imposes a boundary condition on the local vacuum modes

Question	Answer
Is there a reproducible non-sin(θ) component in the QF configurations?	**Sign reproducible, magnitude not**
Is there a reproducible component that survives different analysis methods/angles?	**Internal consistency across analyses of the same data; magnitude unresolved**
Has QF itself been demonstrated rather than an unusual magnetic-geometry effect?	**Not yet**

For details of tests and other supporting documents, see README.txt in
https://drive.google.com/drive/folders/1kyX9nqq-aMQAfwHtXjgVs02RM9rtdCLb?usp=drive_link

© 2026 Mikolaj Baczynski mikolaj.bzk@gmail.com

Vacuum Energy (Event Analysis)

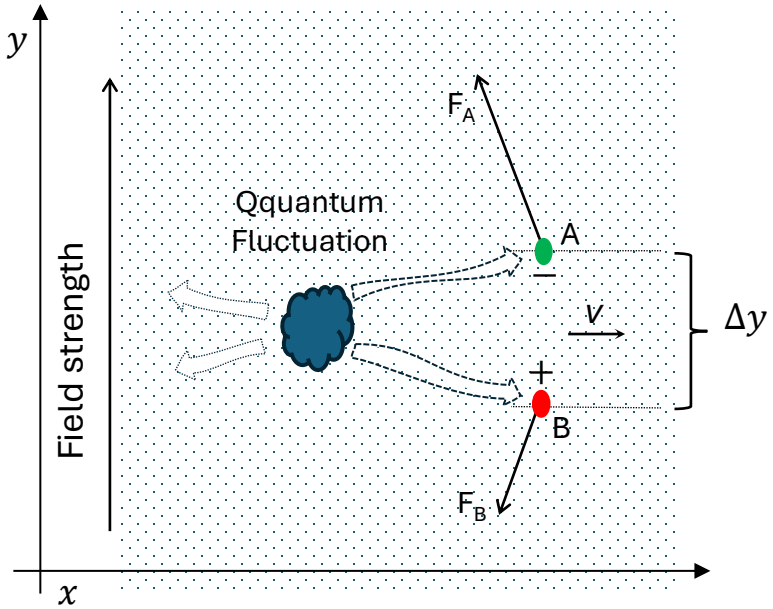

$$\Delta x \Delta p \geq \frac{\hbar}{2} \Rightarrow \Delta x = \frac{\hbar}{2p} = \frac{h}{4\pi p}$$

$$\Delta y = 2\Delta x$$

Velocities at points A and B:

Massless particles:

$$v = c$$

Particles with mass:

$$E = EK + E_0 = \frac{mc^2}{\sqrt{1 - \frac{v^2}{c^2}}}$$

$$v = c\sqrt{1 - \left(\frac{mc^2}{E}\right)^2}$$

Figure 2. Particle positions and velocities

As shown in Figure 2. particle velocities depend on energy and mass. Particle position is governed by the Uncertainty Principle. Given the speed v, and the separation distance Δy, the forces can be obtained as follows:

Using de Broglie wavelength λ :

$$\Delta x \Delta p \geq \frac{\hbar}{2} \Rightarrow \Delta x = \frac{\hbar}{2p} = \frac{h}{4\pi p} = \frac{h\lambda}{4\pi h} = \frac{\lambda}{4\pi}$$

$$\rho_{\text{vac}} = \frac{E}{\Delta x^3} = \frac{hc}{\lambda}\frac{(4\pi)^3}{\lambda^3} = \frac{hc(4\pi)^3}{\lambda^4} \Rightarrow \lambda = \left(\frac{hc(4\pi)^3}{\rho_{\text{vac}}}\right)^{1/4}$$

$$\Delta x = \frac{1}{4\pi}\left(\frac{hc(4\pi)^3}{\rho_{\text{vac}}}\right)^{1/4} = \left(\frac{hc}{4\pi\rho_{\text{vac}}}\right)^{1/4} \quad \boldsymbol{\Delta y = 2\Delta x}$$

$$\vec{F} = qv\vec{B}sin(\theta);\ \theta = 90°, \Rightarrow \vec{F} = ev\vec{B} = ec\frac{\mu_0 \vec{m}}{2\pi d^3}$$

$$\vec{B}_A = \frac{\mu_0 \vec{m}}{2\pi} \cdot \frac{1}{r_A{}^3} \Rightarrow \frac{\mu_0 \vec{m}}{2\pi} = \vec{B}_A \cdot r_A{}^3 \quad \vec{B}_B = \frac{\mu_0 \vec{m}}{2\pi} \cdot \frac{1}{r_B{}^3} = \vec{B}_A \cdot r_A{}^3 \cdot \frac{1}{(r_A + \Delta y)^3}$$

$$\vec{F}_A - \vec{F}_B = ec\left(\vec{B}_A - \vec{B}_B\right) = ev\vec{B}_A\left(1 - \frac{r_A{}^3}{(r_A + \Delta y)^3}\right)$$

Note:

- the QF force direction depends on field gradient not the sing of charge; A/B particles pairs can be +/- or -/+; with opposite $\boldsymbol{v}$
- The force and vacuum-energy-density estimates use the massless case ($v = c$). The massive-particle energy and speed relations shown above are included only for completeness

© 2026 Mikolaj Baczynski mikolaj.bzk@gmail.com

Vacuum Energy (estimating QF)
Speculative Engineering Approach

Earth's Field Not Included in the Model!

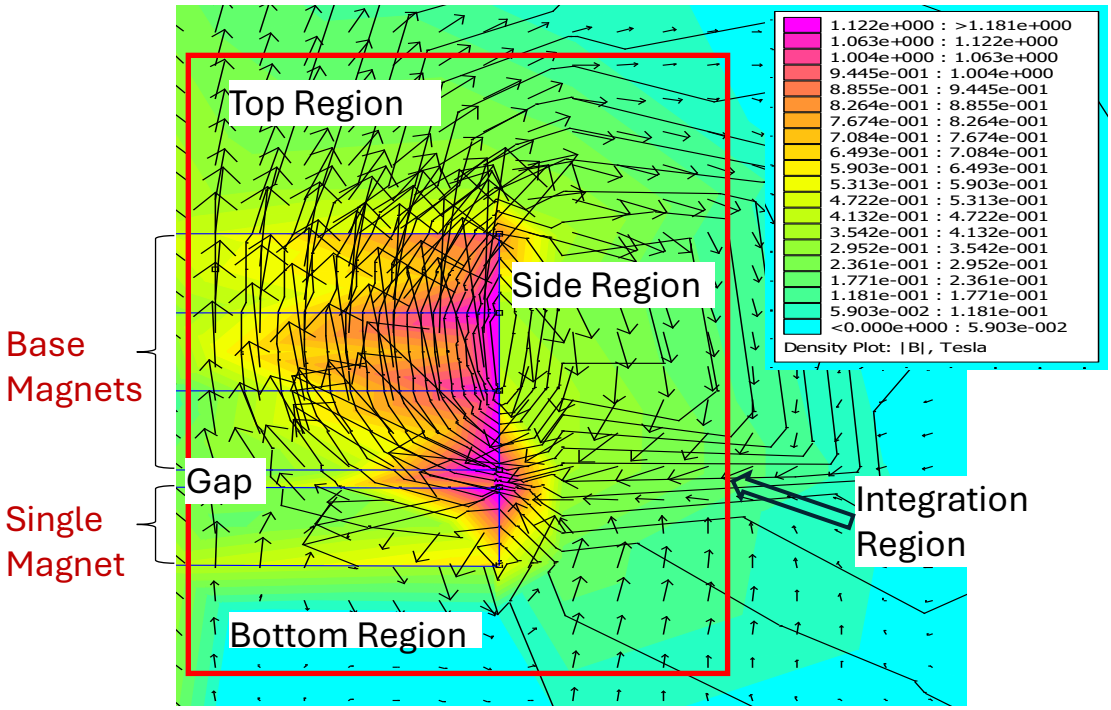

Given $\vec{F}_A - \vec{F}_B = ev(\vec{B}_A - \vec{B}_B)$; $F_T = \iiint_V (f_A - f_B) \Rightarrow \sum_1^N (F_A - F_B) = N\,(F_A - F_B)$ where N is the number of fluctuations in the region of integration based on the vacuum energy density ρ_{vac}.

The following table was obtained, by calculating the field gradient, ΔBr, in each region and plugging in, **arbitrary**, vacuum energy density

Example of forces given $\boldsymbol{\rho_{vac}}$ of 2.60E-09[J/m^3] with fluctuations producing massless pairs				
Region	Volume [m^3]	Average ΔBr [T/m]	QF [N]	N [number of fluctuation pairs]
Gap	5.43E-07	-9.06E+01	7.77E-07	4.44E+06
Side	4.02E-01	1.43E-06	-9.07E-09	3.28E+12
Bottom	2.65E-04	1.28E-01	-5.35E-07	2.16E+09
Top	2.65E-04	-6.11E-01	2.56E-06	2.16E+09
		QF Total	**2.79E-06**	

The above table generated by calling: qf_dBy_get(2.6E-9, 0) in qtCalc.lua

© 2026 Mikolaj Baczynski mikolaj.bzk@gmail.com

Vacuum Energy (assumptions)
Speculative Engineering Approach

What "momentum into vacuum" means: By *momentum into vacuum* I mean a momentum exchange between the magnet assembly and the transient fluctuation pairs that briefly populate the field-gradient region. The pair is the receiving degree of freedom: in this model the gradient would exert the net force F_A − F_B on the ± members of a pair, the pair would carry off that net momentum, and the assembly would recoil by an equal and opposite amount — that recoil being what the balance measures. At the instant of interaction, momentum is conserved by Newton's third law — nothing here requires conservation to be broken.

Assumptions (unvalidated toy model):

- *Species/coupling:* applies charge e and F = e·v·B to the pairs; m = 0 fixes the kinematics (v = c) but does not identify a species or justify the coupling — assumed.
- *Size:* $\Delta x = \lambda/(4\pi)$ from saturating $\Delta x \cdot \Delta p = \hbar/2$ with $p = h/\lambda$, and $\Delta y = 2\Delta x$. Saturation and this size–energy link are modelling choices, not consequences of the uncertainty inequality.
- *Density/counting:* ρvac is one pair's energy $E = hc/\lambda$ per cell Δx^3 (a per-pair density), with $N = V/\Delta x^3$; the 4π factors define the cell, they are not measured.
- *Force:* the pair lifetime is not modelled — N·(F_A − F_B) is treated as a steady, not transient, force.

Chosen, not measured: $\rho_{vac} = 2.6 \times 10^{-9}$ J/m^3 was selected so the total (≈ 2.79 μN) matches the observed scale; agreement from a chosen input is not a prediction or measurement of vacuum energy — only the density this model would require.

Conservation: the pair is transient; if it recombines locally and symmetrically, the impulse is returned and no steady force survives, thus, a net force requires the momentum to be carried off or radiated before recombination — an outflow this work does not model. A complete account must name the final reservoir (radiated field, net field momentum, or other vacuum modes) and show the per-event impulse survives a recombination cycle; until then "momentum into vacuum" is a proposed exchange channel, not a closed balance.

Numerical status. The vacuum-estimate gradient ΔBr is read directly from the same FEM field solution as the force model — a node-to-node/point-to-point Br gradient is averaged over, a region. There is no physical normalization only gradient-to-force mapping:

```
region_QF = e * v * -dBr_avg*2*plank_dx * region_N * qf_factor
```

with qf_factor = $4/\pi^2$. This scaling factor's physical normalization is unvalidated and the gradient's mesh-convergence was likewise not characterized.
Other than using the same node solution, there is no connection with, or reliance on, the way magnetic moment was calculated in estimating the interaction with the Earth's magnetic field (pp.13–14).

© 2026 Mikolaj Baczynski mikolaj.bzk@gmail.com

Field Nulling with Helmholtz Coils (still to be performed)

Classical field-coupling and QF results are identical in Earth's field:

- Classical coupling requires an external field (torque = m·B_ext)
- QF is driven by the assembly's own gradient and doesn't need any external field
- In Earth's field you can shrink the field's projection by changing angle, but you can never null the field itself or reverse it
- Helmholtz coils can null the modeled external field, and so test and reduce the specified classical coupling — not guaranteed to eliminate every conventional contribution

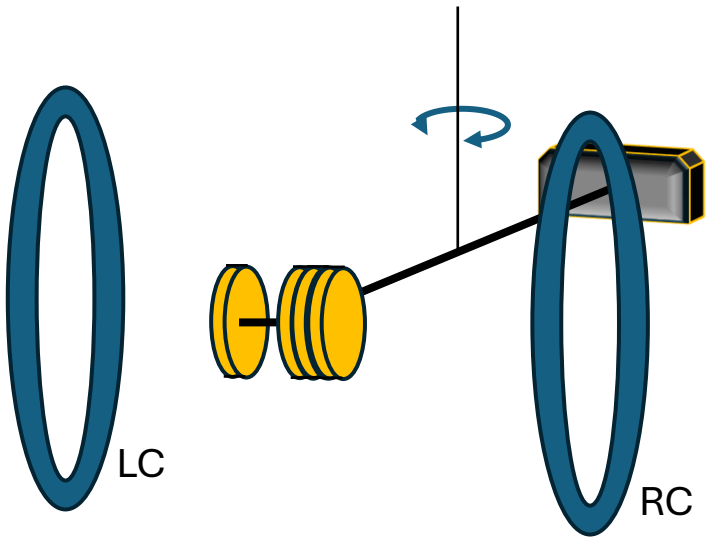

Coil setup:

- Left-Right (LC-RC) coils null the horizontal component B_h
- Nulling B_v component is of little value

Left-Right (LC-RC) coils is sufficient:

- Align the coils North-South
- **F_noQF must be < 1**[μN] for both NS and SN

© 2026 Mikolaj Baczynski mikolaj.bzk@gmail.com

Design Details of Helmholtz Coils

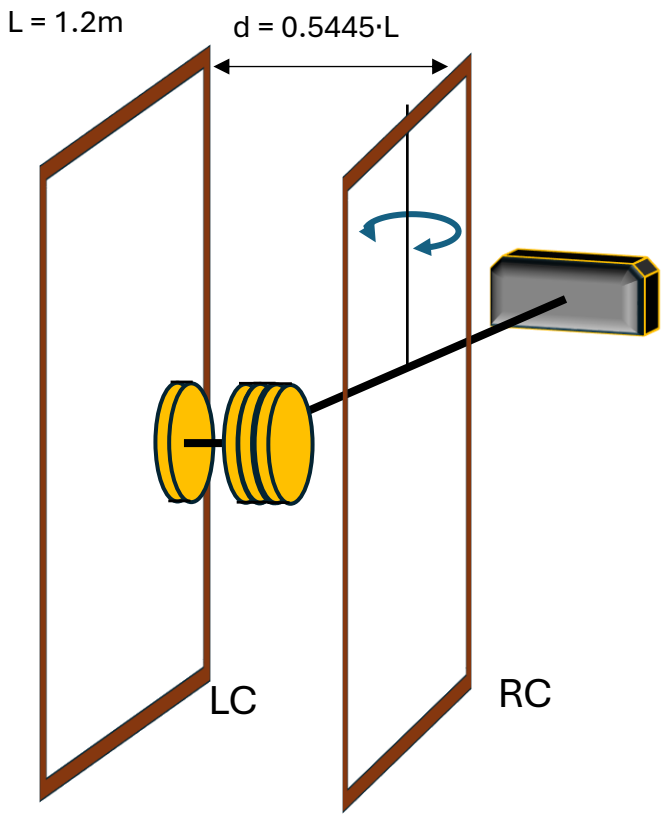

Fixed geometry & null region

Parameter	Value
Coil shape / side	Square, 1.20 m
Separation (critical)	0.653 m (0.5445 L), hold to ±10 mm
Field constant	1.357 μT/A per turn → k = 1.357 · N μT/A
<1 μN null region (at optimal spacing)	±53 mm axial × ±66 mm transverse × ±66 mm vertical (≈106 × 132 × 132 mm)
Twist tolerance (÷0.40 m arm)	±7.6° (axial) to ±9.5° (transverse)
Margin over assembly (±15 mm)	~3.5× on every axis

© 2026 Mikolaj Baczynski mikolaj.bzk@gmail.com